

# Dark Energy from Large Extra Dimensions

---

**Kimmo Kainulainen and Daniel Sunhede**

*Dept. of Physics, University of Jyväskylä,  
P.O.Box 35 (YFL), FIN-40014 University of Jyväskylä*

**ABSTRACT:** We explore in detail a model by Albrecht, Burgess, Ravndal and Skordis, where a radion field from two compact extra dimensions gives rise to quintessence in our 4-dimensional world. We show that the model can give rise to other types of cosmologies as well, some more akin to  $k$ -essence and also variants of phantom dark energy. In our realization of the scenario the radius stabilization arises not from the Casimir potential, but from quantum corrections to the effective 4D Ricci-scalar. We show that the new stabilization scheme can be implemented in a converging perturbation expansion for the effective 4D action without fine tuning. We then show that various constraints nearly determine the expansion parameters, and give an example of a quintessence-type cosmology consistent with observations. We show that the upcoming SNAP-experiment would easily distinguish the present model from a constant  $\Lambda$  model with an *equal* amount of dark energy, but that the SNAP-data alone will not be able to distinguish it from a  $\Lambda$  model with about 5% less dark energy.

**KEYWORDS:** Cosmology, Dark Energy, Quintessence.

## 1. Introduction

The discovery that the expansion of the universe is accelerating implies the existence of an extremely small, but non-zero vacuum energy density. In summary, the observations have led to a new cosmological concordance model, according to which [1]  $\Omega_{\text{tot}} = 1.02 \pm 0.02$ ,  $\Omega_{\Lambda} \approx 0.73$ , and  $\Omega_m \approx 0.27$ . That is, the universe is flat and dominated by a “dark energy” component  $\Omega_{\Lambda}$  which has an equation of state close to that of a bare cosmological constant today. The physical nature of the dark energy component is not known, but according to the popular *quintessence* scenario [2–4], it corresponds to energy stored into a classical background scalar field with some very particular properties. An interesting class of quintessence models can be characterized by a Lagrangian [3–6]

$$\mathcal{L} = \frac{1}{2}(\partial\chi)^2 - V_p(\chi)e^{-\lambda\chi}, \quad (1.1)$$

where  $V_p(\chi)$  is some power-law modification to the dominant exponential factor. A desirable feature of such exponential potentials is that a small change in the field value  $\chi$  can cause a large change in the energy density  $\rho_{\chi}$ . Moreover, they often allow scaling solutions, where the kinetic and potential energies of  $\chi$  maintain a fixed ratio, leading to a constant equation of state parameter  $w_{\chi}$  and to  $\rho_{\chi}$  scaling exactly as a power of the scale factor. This in particular makes it possible for the quintessence field to mimic a cosmological constant.

Generic quintessence scenarios often rely on an *ad. hoc.* quintessence field with some suitably adjusted potential. A more complete physical theory should explain the origin of the – possibly effective – quintessence field and naturally predict the exponential form of its potential. Remarkably, these requirements are met in a model with two large extra dimensions, put forward by Albrecht, Burgess, Randall and Skordis [7–9]. In the ABRS model the quintessence field corresponds to the radion mode, which after a toroidal compactification of the 6-dimensional manifold shows up as an effective Jordan-Brans-Dicke field in the residual 4-dimensional action in the Einstein frame. There are two central observations that make the 6D model special: First, the dimensionality of the model allows adding a light bulk scalar field  $\phi$  with renormalizable cubic interactions, which then induce logarithmic corrections to the radion potential. These corrections are crucial for the large radius stabilization mechanism, both in the original ABRS model and in its present modification. Second, the cosmological constant can arise in a parametrically natural way from the Casimir potential  $U \sim U_0/r^4$  in models with large extra dimensions. Indeed, setting  $U \sim 10^{-120} M_{\text{Pl}}^4$  with  $U_0 \sim 1$  requires a radius  $r \sim (10^{-3}\text{eV})^{-1}$ . In a model with  $n$  equally large extra dimensions, the apparent and the fundamental gravity scale are related by  $M_{\text{Pl}}^2 = M_b^{2+n}r^n$ . Thus in a 6D model, the naturalness condition  $U_0 \sim 1$  corresponds to weak scale  $M_b \sim 1 \text{ TeV}$ , whereas already for  $n = 3$  one would need a way too low scale  $M_b \sim 1 \text{ GeV}$ . Seen the other way around, setting the fundamental scale to TeV in a model with  $n > 2$ , would require fine-tuning  $U_0$  to extremely small values ( $U_0 \sim 10^{-20}$  for  $n = 3$ ).

The present model is strongly confronted by the existing astrophysical constraints, and most notably by the precision tests of General Relativity in the solar system [10]. GR-constraints were already considered by the authors of ref. [8], but our results differ from theirs; in fact we found that they rule out the original scenario when correctly accounted for.

The problem arises from the fact that the perturbative loop corrections, which were treated as small quantities in ref. [8], actually must be of order unity. We point out that technically the effective one-loop corrections can be large, while higher corrections are negligible, if only the corrections come from *many* independent very weakly coupled fields  $\phi_i$ . While this realization allows for a converging perturbative expansion, it turns out to invalidate the original radius stabilization mechanism based on the Casimir potential. Moreover, one is not allowed to expand any of the expressions arising from the action in the first order loop corrections. Luckily this turns out to give rise to a new stabilization mechanism for the radius: If the one loop correction to the 4D Ricci scalar  $R_{\hat{g}}$  is negative, then the scaling function  $A(r)$  must become zero and eventually negative for logarithmically large radius  $r$ . This root of the  $A(r)$ -function introduces a confining singularity into the effective radion potential in the Einstein frame. This mechanism requires no fine-tuning from the model building point of view, is more robust than the one relying on the Casimir potential, and moreover, almost automatically makes the model compatible with the GR-constraints.

Astrophysical and theoretical constraints nearly fix the relevant model parameters. Moreover, for a given set of parameters, there is practically a unique set of initial conditions that can give rise to correct values for the cosmological parameters today. We present a particular quintessence-like solution which obeys all constraints, starting from time before nucleosynthesis until today. We then argue that our model makes a generic prediction for the evolution of the equation-of-state parameter  $w(z)$ , which in principle makes it distinguishable from a flat constant  $\Lambda$ -cosmology. We then show that the sensitivity of the forthcoming SNAP-experiment [11] should be good enough to separate our model from a constant  $\Lambda$  model with *equal* amount of dark energy today. However, the SNAP-data [12] alone will not be able to break a degeneracy between our model and a  $\Lambda$  model with slightly different amount of dark energy (about 5% less).

The new perturbative scheme for the effective model parameters introduces a very complicated structure for the kinetic term of the Jordan-Brans-Dicke field in the Einstein frame. Even with the little room one has to play after applying the constraints, it is in fact possible to arrange model parameters such that this term becomes very large and possibly singular, or even negative. In either of the former cases the model classifies rather as a  $k$ -essence than a quintessence scenario, and in the latter it gives rise to variants of recently introduced phantom cosmologies [13]. In this paper we mostly concentrate on non-phantom models. While we do give some examples of parametrizations leading to phantom cosmologies, it is not clear to us whether it is possible to make these scenarios compatible with observations.

The paper is organized as follows. We begin by reviewing the basic ABRS model and its reduction to an effective 4D gravity theory in section 2. In section 3 we discuss how the effective 4D theory relates to other dark energy models including  $k$ -essence, quintessence and phantom cosmology. We also derive an effective action for the model in terms of the Jordan-Brans-Dicke field  $\chi$  in the Einstein frame, and from it the coupled cosmological evolution equations for  $\chi$  and various density components. In section 4 we outline a perturbatively reliable scheme with a new mechanism for the radius stabilization and in section 5 we derive constraints on model parameters arising from various theoretical and astrophys-

ical considerations. In section 6 we present a realistic cosmological evolution from times before nucleosynthesis until present that satisfies all observational constraints. We also compute the prediction of the model for the supernovae magnitude-redshift relation and compare it with cosmological constant models. Finally, section 7 contains our summary and the conclusions.

## 2. The ABRS Model

Albrecht *et al.* proposed a brane world scenario in which our  $(3+1)$ -dimensional space is a brane embedded in a six-dimensional bulk space [7, 8]. All standard model fields are confined to the four-dimensional brane while gravity propagates in all six dimensions. The scale of physics on the brane is assumed to be of weak scale,  $M_b \sim 1$  TeV. The observed 4D gravitational coupling in this model is<sup>1</sup>  $M_{\text{Pl}} \equiv (8\pi G)^{-1/2} \sim M_b^2 r \sim 10^{18}$  GeV, which then implies a large radius of extra dimensions  $1/r \sim 10^{-3}$  eV. This corresponds to the dimensionless parameter  $M_b r \sim 10^{15}$ .

The full action of the theory can be divided into two terms,  $S = S_{\text{B}} + S_{\text{b}}$ , corresponding to the bulk and the brane contributions respectively. The leading part of the bulk action is

$$S_{\text{B}} = \frac{M_b^4}{2} \int d^4x d^2y \sqrt{-\mathcal{G}} (\mathcal{R} + \mathcal{L}(\phi)) , \quad (2.1)$$

where  $\mathcal{R}$  is the scalar curvature built from the six-dimensional metric  $\mathcal{G}_{MN}$  and  $\mathcal{L}(\phi)$  represents the (possibly multi-field) Lagrangian for the six dimensional  $\phi^3$ -theory. The detailed form of the brane action is not important; the crucial part is that it only depends on the *four*-dimensional metric  $\hat{g}_{\mu\nu}$ :

$$S_{\text{b}} = \int d^4x \sqrt{-\hat{g}} \mathcal{L}_{\text{m}}(\hat{g}_{\mu\nu}, \dots) . \quad (2.2)$$

All matter fields, denoted by ellipses in  $\mathcal{L}_{\text{m}}$ , are trapped on the brane and do not carry stress-energy into the extra dimensions. The cosmological constant  $\Lambda$  is assumed to vanish due to some six-dimensional symmetry. Further, we assume that the six-dimensional metric has a block-diagonal structure:

$$\mathcal{G}_{MN} = \begin{bmatrix} \hat{g}_{\mu\nu}(x) & 0 \\ 0 & \varrho^2(x) h_{mn}(y) \end{bmatrix} . \quad (2.3)$$

That is, the six-dimensional space-time manifold is assumed to be such that each point of the brane is connected to a two-dimensional surface with a metric  $h_{mn}$ , such that the size of the extra dimensions,  $\varrho(x) = M_b r(x)$ , is allowed to vary as a function of the position in the brane.

---

<sup>1</sup>Note that we are using this somewhat unconventional definition of the Planck mass in order to be more compatible with the refs. [7–9]. Note however, that we are using a positive signature for the metric  $(+---)$ , whereas ABRS used a negative signature  $(-+++)$ .

## 2.1 Effective 4D Theory

We are obviously interested in the effective four dimensional theory on the brane on large scales. It can be obtained from Eqns. (2.1-2.2) via standard dimensional reduction. Indeed, integrating out the extra spatial dimensions at the tree-level one finds an effective action [7]:

$$S_{\text{eff}} = \int d^4x \sqrt{-\hat{g}} \left[ \frac{M_b^4 r^2}{2} \left( R_{\hat{g}} - 2 \left( \frac{\partial r}{r} \right)^2 + \frac{1}{r^2} \int d^2y \sqrt{h} R_h \right) + \mathcal{L}_m(\hat{g}) \right], \quad (2.4)$$

where  $R_{\hat{g}}$  and  $R_h$  represent the scalar curvature arising from  $\hat{g}_{\mu\nu}$  and  $h_{mn}$ , respectively, and the normalization of  $h$  is chosen such that  $M_b^2 \int d^2y \sqrt{h} \equiv 1$ . Action (2.4) still explicitly depends on the extra dimensions via the curvature term  $R_h$ . Choosing the topology of the extra dimensions to be flat and periodic (torus), the curvature  $R_h$  vanishes however, leaving out only an effective 4D Ricci scalar and a kinetic term for  $r$ .

The tree-level theory (2.4) is further modified by quantum corrections. These include both renormalization of the kinetic terms and an introduction of a no-derivative potential  $U(r)$  to the effective theory. For the toroidal compactification the leading term of the potential is contributed by the Casimir energy, and is given by [7]:

$$U = \frac{U_0}{r^4} + \dots \quad (2.5)$$

The crucial part in the theory of Albrecht *et al.* is the inclusion of the scalar field into the bulk with renormalizable cubic interactions. The renormalizability ensures that scalar field quantum corrections are logarithmic (instead of power-like) in the cut-off given by the scale  $r$ . Hence, the corrected form of the effective 4D theory may be parametrized as

$$S_{\text{eff}} = \int d^4x \sqrt{-\hat{g}} \left[ \frac{M_b^4 r^2}{2} \left( A(r) R_{\hat{g}} - 2B(r) \left( \frac{\partial r}{r} \right)^2 \right) - C(r) \frac{U_0}{r^4} + \mathcal{L}_m(\hat{g}) \right], \quad (2.6)$$

where to lowest order

$$A(r) \approx 1 + a \log M_b r, \quad (2.7)$$

$$B(r) \approx 1 + b \log M_b r, \quad (2.8)$$

$$C(r) \approx 1 + c \log M_b r. \quad (2.9)$$

Here  $a$ ,  $b$ , and  $c$  are some unknown but small parameters proportional to the dimensionless coupling constant,  $\epsilon \equiv g^2/(4\pi)^3$ . It is remarkable that the form (2.6) arises basically from two simple assumptions; that the topology of extra dimensions form a torus, and the presence of renormalizable scalar theory in six dimensions.

## 2.2 ABRS Radius Stabilization

The original ABRS argument for large radius stabilization of the compactified dimensions was based on the particular form of the quantum corrected Casimir potential [6, 7, 14] in equation (2.6):

$$U(r) = U_0 M_b^4 \left( \frac{1}{M_b r} \right)^4 [1 + c \log(M_b r)]. \quad (2.10)$$

$U(r)$  always has a runaway minimum at  $r \rightarrow \infty$ . However, if  $c$  is negative it develops another minimum at finite, but exponentially large scale (in comparision with the microscopic scale  $l = M_b^{-1}$ ):

$$M_b r \approx \exp\left(\frac{1}{4} + \frac{1}{|c|}\right). \quad (2.11)$$

Fixing  $M_b r$  to the desired value  $\sim 10^{15}$  indeed sets the scale of radiative corrections to a small and perturbatively natural value  $|c| \sim \epsilon \sim 1/50$ . This simple argument neglects the coupling between the radius and the 4D metric in Eqn. (2.6) however. In reality one cannot make this assumption, and it will turn out that the other radiative corrections, and the  $A$ -term in particular, will play a crucial role in later developments.

### 3. Quintessence, $k$ -essence or Phantom Energy?

We have so far written the 4D model in the so called Jordan frame, where the metric  $\hat{g}_{\mu\nu}$  is not canonically normalized. The cosmology is far more transparent in the Einstein frame (denoted below by a metric  $g_{\mu\nu}$  without a hat), where the gravitational action has the usual definition:

$$\frac{M_b^4 r^2}{2} A R_{\hat{g}} \equiv \frac{M_b^2}{2} R_g + \text{additional terms}. \quad (3.1)$$

Since schematically  $R_g \propto g_{\mu\nu}^{-1}$ , Eqn. (3.1) implies the conformal transformation

$$\hat{g}_{\mu\nu} \equiv \frac{g_{\mu\nu}}{(M_b r)^2 A}. \quad (3.2)$$

It would be possible to continue our analysis in the Einstein frame maintaining the radius  $r$  as a variable in the theory. However, is more instructive to introduce an effective field  $\varphi$  (not to be confused with the 6D scalar  $\phi$ ) defined simply as the logarithm of the radius:

$$\varphi \equiv \log(M_b r). \quad (3.3)$$

With these definitions, the action (2.6) can be recast as

$$S_{\text{eff}} = \int d^4x \sqrt{-g} \left[ \frac{M_b^2}{2} R_g + \frac{1}{2} k^2(\varphi) (\partial\varphi)^2 - V_E(\varphi) + \mathcal{L}_m(g, \varphi) \right], \quad (3.4)$$

where

$$V_E(\varphi) \equiv M_b^4 U_0 \frac{1 + c\varphi}{(1 + a\varphi)^2} e^{-8\varphi}. \quad (3.5)$$

and

$$k^2(\varphi) \equiv M_b^2 \left[ \frac{3}{2} \left( 2 + \frac{a}{1 + a\varphi} \right)^2 - \frac{2(1 + b\varphi)}{1 + a\varphi} \right]. \quad (3.6)$$

Note that we have *not* expanded any the above expressions in perturbative parameters; it will later become clear why this indeed is the sensible thing to do. Written in the form (3.4) our effective theory has obvious resemblance with some popular toy models studied earlier in the literature. First, if the radiative corrections were neglected (or they are negligibly small so that effectively  $a, b, c \simeq 0$ ) the potential reduces to a pure exponential and the

kinetic energy becomes canonical apart from a constant scaling. In this limit our theory thus becomes equivalent with the original *quintessence* scenario [15]. We shall see later that the model, despite the modifications due to radiative corrections, does lead to some quintessence-like cosmological solutions.

In general, the function  $k^2(\varphi)$  gives rise to a non-canonically normalized kinetic term for  $\varphi$ , which is the trademark of another class of dark energy models called *k-essence* [16,17]. In particular our model bears similarity to mixed *k*-essence - quintessence models discussed in ref. [16]. Observe in particular that in the Planck era, *i.e.* when  $r \sim M_b^{-1}$  or  $\varphi \sim 0$  we have  $k^2(\varphi) = 4M_b^2$  and  $V(\varphi) = U_0 M_b^4$ . Thus the theory (3.4) is natural (contains no arbitrarily small parameters) if only  $U_0 \sim 1$ . This is of course required independently by the naturalness of our underlying model from a field theory point of view, and we shall see later that it does give rise to acceptable cosmologies as well.

It is conceivable that for certain values of the parameters  $a$  and  $b$ , the function  $k^2(\varphi)$  becomes negative. In this case our model corresponds neither to *k*-essence nor to quintessence, but instead exhibits the features of *phantom cosmologies* [13], with an equation-of-state parameter  $w_\varphi < -1$ . (Of course, as was also pointed out in ref. [17], the phantom models could be viewed as forming a particular class of *k*-essence models.) For example, it would seem quite possible that our model initially starts as quintessence or *k*-essence, and later in time changes its behaviour to a phantom cosmology, or vice versa. We shall show later that such behaviour indeed can arise in the present context with natural values of the model parameters. However, for the most part of the paper we will concentrate to the case where  $k^2(\varphi) > 0$ .

Let us finally note that the conformal transformation (3.2) between the Einstein and Jordan metrics is singular at  $A(r_*) = 0$ , and that changing the sign of  $A$  effectively reverses the signature of the Einstein metric. At the singular point all masses apart from the Planck mass diverge in the Einstein frame, and even stranger yet, should  $A$  become negative, all brane field masses would become imaginary (see equation (3.16) below. That is, all normal matter would become tachyonic! Perhaps fortunately these considerations appear mostly academic, as we shall see that it is practically impossible for any classical evolution starting from a radius smaller than  $r_*$  to move past the singularity, hence keeping the radion confined to values below  $r_*$  at all times.

### 3.1 Non-Phantom Cosmologies

When  $k^2(\varphi) > 0$  we can make a further change of variables such that the kinetic term has the standard canonical form [16]. In this case our theory belongs roughly to the class of *k*-essence and quintessence models. The difference between the latter two is that in *k*-essence the behaviour of the field is driven by its non-canonical kinetic term (in a pure *k*-essence the potential is actually vanishing [17]), whereas in quintessence the desired behaviour follows from the special form of the potential. We find that our model can at times behave as quintessence and at others as *k*-essence, as well as show some characteristics not typical to either of them. Indeed, introducing

$$\chi = K(\varphi) \quad \text{with} \quad k(\varphi) = \frac{\partial K(\varphi)}{\partial \varphi} \quad (3.7)$$

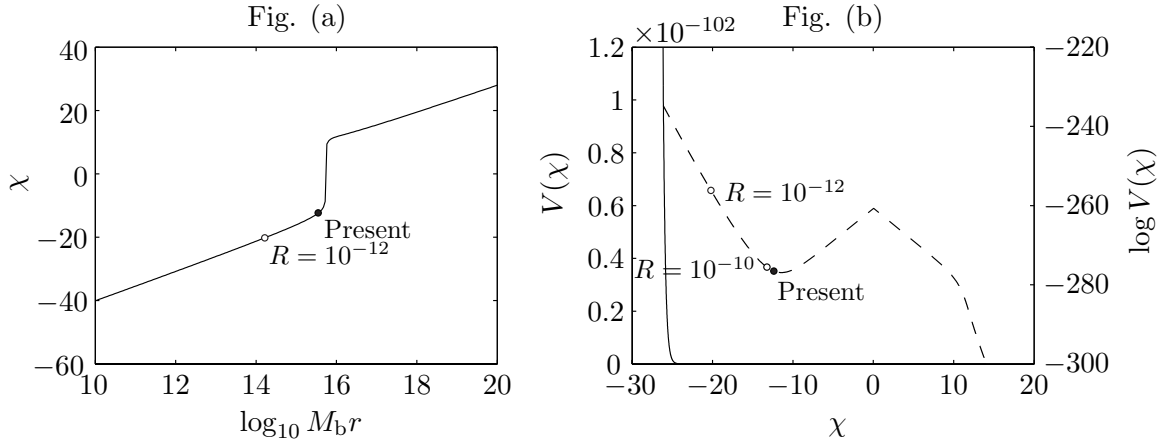


**Figure 1:** (a)  $\chi$  in terms of  $\log(M_b r) = \varphi/\log 10$  for the case  $a = -0.0276$  and  $b = -0.031$ . (b) The potential  $V(\chi)$  for the same  $a$  and  $b$ , and for  $U_0 = 2.68$  and  $c = 0$ . The dashed line represents  $\log V(\chi)$ . The open and closed circles represent the instantaneous values of the field and the corresponding value of the potential at given times (labeled by the value of the scale factor) in the past and at present ( $R = 1$ ) for a particular explicit solution of the equations of motion to be discussed in detail below.

we get the effective action

$$S_{\text{eff}} = \int d^4x \sqrt{-g} \left[ \frac{M_b^2}{2} R_g + \frac{1}{2} (\partial\chi)^2 - V(\chi) + \tilde{\mathcal{L}}_m(g, \chi) \right], \quad (3.8)$$

where  $V(\chi) \equiv V_E(\varphi) = V_E(K^{-1}(\chi))$ .

We have found an analytic expression for  $\chi$  in terms of  $\varphi$ , and eventually in terms of  $M_b r$ , from Eqns. (3.6), (3.7) and (3.3). It is rather complicated however, and we defer the explicit solution to the appendix A. We plot the result for  $\chi$  as a function of  $\log_{10} M_b r = \varphi/\log 10$  in Fig. (1a). The dependence is smooth and linear except at a point where the derivative  $d\chi/d\varphi$  becomes very large (in fact infinite). As a result, the potential  $V$  is roughly exponential also as a function of  $\chi$  away from the singularity, *i.e.* automatically of the desired type for quintessence (cf. Eqn. (1.1)). We plot  $V(\chi)$  for a representative choice of model parameters in Fig. (1b).  $V(\chi)$  is indeed exponential for  $\chi \lesssim -12$ . Moreover it has a minimum that leads to a radius stabilization, which here corresponds to  $M_b r \approx 3.5 \times 10^{15}$ . Note that the potential minimum is situated very close to the  $d\chi/d\varphi$ -singularity in  $r$ . This is so because the  $\varphi$ -scale is very strongly condensed with respect to  $\chi$  near singularity. We shall return to this and the other features seen in the potential function shortly.

### 3.2 The Evolution Equations

The action (3.8) forms the basis of the cosmology to be studied in the rest of the paper. Taking a variation with respect to the field  $\chi$  leads to an equation of motion

$$\ddot{\chi} + 3H\dot{\chi} + V'(\chi) + \frac{\eta(\chi)}{M_b} T_\mu^\mu = 0, \quad (3.9)$$

where  $H$  is the Hubble expansion rate. The explicit form of the derivative of the potential  $V'(\chi) \equiv \partial V / \partial \chi$  is

$$V'(\chi) = M_b^3 U_0 \frac{1}{(M_b r)^8} \frac{cA - 2aC - 8AC}{A^2 \sqrt{\frac{3}{2}(2A + a)^2 - 2AB}}, \quad (3.10)$$

and the coupling function  $\eta$  is given by

$$\eta(\chi) = -\frac{A + a/2}{\sqrt{\frac{3}{2}(2A + a)^2 - 2AB}}. \quad (3.11)$$

These are all exact expressions (at the one loop) and to evaluate them as a function of  $\chi$ , one needs the inverse of the transformation (3.7), *i.e.* for example  $A = 1 + aK^{-1}(\chi)$ . Finally,  $T_{\mu\nu}$  is the stress-energy tensor of radiation and matter, but since matter is pressureless and  $p = \frac{1}{3}\rho$  for radiation, we have simply  $T_\mu^\mu = \rho_m$ .

The Hubble parameter and the  $\eta$ -term couple the evolution of the  $\chi$ -field to the evolution of the ordinary radiation and matter components. Varying the action (3.8) with respect to the metric yields the Friedmann equations for the flat, homogenous and isotropic brane cosmologies:

$$3M_b^2 H^2 = \rho, \quad (3.12)$$

$$-2M_b^2 \dot{H} = \rho + p, \quad (3.13)$$

where  $H \equiv \dot{R}/R$  as usual and  $\rho$  and  $p$  are the total energy and pressure densities:

$$\rho = \rho_m + \rho_r + \rho_\chi \quad (3.14)$$

$$p = p_r + p_\chi. \quad (3.15)$$

At this point it is important to note that because of the rescaling of the metric (3.2), all masses in the Einstein frame get scaled compared to the Jordan frame. This can be deduced from the scaling of the rest mass of a particle:  $m_{\text{Jordan}}^2 \equiv \hat{g}^{\mu\nu} p_\mu p_\nu = (M_b r)^2 A g^{\mu\nu} p_\mu p_\nu \equiv (M_b r)^2 A m_{\text{Einstein}}^2$ . That is:

$$m_{\text{Einstein}} = \frac{m_{\text{Jordan}}}{M_b r \sqrt{A}}. \quad (3.16)$$

Hence, setting  $M_b = 1$  corresponds to using TeV units in the Jordan frame, but Planck units in the Einstein frame. However, note that  $M_b r$  has the same numerical value in both frames since  $r$  scales oppositely to  $M_b$ . Using Eqn. (3.16) together with the usual scale-factor dependence of the 3-volume on the brane, one finds

$$\rho_m = \rho_{m0} \left( \frac{R_0}{R} \right)^3 \frac{M_b r_0 \sqrt{A_0}}{M_b r \sqrt{A}}, \quad (3.17)$$

where  $R$  denotes the scale factor and  $R_0$ ,  $r_0$  and  $A_0$  refer to the present day values of the quantities. This non-trivial evolution of the matter density as well as the coupling term proportional to  $\eta$  in the equation of motion, Eqn. (3.9), differentiate our model from simple toy models for quintessence and  $k$ -essence. In contrast to pressureless matter, the radiation

density  $\rho_r$  evolves normally ( $\rho_r \propto R^{-4}$ ). This can be seen to arise as a result of the zero rest mass of the photon. Including the contributions from the  $\chi$ -field one eventually finds:

$$\rho = \rho_{m0} \left( \frac{R_0}{R} \right)^3 \frac{M_b r_0 \sqrt{A_0}}{M_b r \sqrt{A}} + \rho_{r0} \left( \frac{R_0}{R} \right)^4 + \frac{1}{2} \dot{\chi}^2 + V(\chi), \quad (3.18)$$

$$p = p_{r0} \left( \frac{R_0}{R} \right)^4 + \frac{1}{2} \dot{\chi}^2 - V(\chi). \quad (3.19)$$

Equations (3.9-3.11) together with the Friedmann equations (3.12-3.13) and the explicit expressions for density and pressure (3.18-3.19), form a complete set of equations for the evolution of  $\chi$  (or equally  $r$ ) and the scale factor  $R$ .

#### 4. Radius Stabilization and Convergence of Perturbation Theory

In section (2.2) we presented an argument for the stabilization of the radius of the extra dimensions based on a particular form of the Casimir potential, Eqn. (2.10). According to Eqn. (2.11) the stabilization with  $M_b r \sim 10^{15}$  is consistent with the perturbative scale  $|c| \sim \epsilon \sim 1/50$ . At first, such a small scale looks perfect for a perturbative treatment of the problem. Reliability of the perturbation theory is indeed necessary for us, because our action (Eqn. (2.6)) and all subsequent formulae for the effective 4D cosmology derived from it in later sections, rely heavily on the effective *one-loop* parametrization of the radiative corrections. There is a fundamental flaw in the above argumentation however, since the actual expansion parameter is not  $\epsilon$ , but

$$\varepsilon \equiv \epsilon \log M_b r. \quad (4.1)$$

Now, reading Eqn. (2.11) the other way around, we see that for  $\log M_b r \gg 1$  it sets  $\epsilon \simeq 1/\log M_b r$ , or equivalently  $\varepsilon \approx 1$ ! Hence, the perturbative expansion appears to be *necessarily* diverging, at least in the case of the potential. But since all corrections originate from the same bulk scalar field  $\phi$  they should all be roughly of same order  $a \sim b \sim c \sim 1/50$ , which renders the entire 1-loop parametrization in (2.6-2.9) useless. In fact the radius stabilization mechanism itself would only seem to work qualitatively at best, and could be destroyed by unknown higher loop and non-perturbative corrections.

It is quite interesting that a similar conclusion follows also from the observational gravity constraints. Avoiding conflict with the general relativity on the solar system scale sets a bound on the coupling between the  $\chi$ -field and matter [10]:

$$\eta^2(\chi_0) < 0.001 \equiv \eta_0^2. \quad (4.2)$$

From Eqn. (3.11) it is then clear that one must have very accurately  $A \simeq -a/2$ . From the one-loop expression  $A = 1 + a \log M_b r$  and the fact that  $\log M_b r$  is large by assumption, we then see that  $a < 0$  and  $|a| \ll 1$ , so that a solution only exists if  $a \log M_b r \simeq -1$ . That is, the one-loop contribution must again balance the tree level one to a high precision. These two arguments seem to cast a serious doubt over the validity of our phenomenological one-loop parametrization of the 4D action.

## 4.1 A Scenario with a Reliable Perturbative Expansion

Fortunately there are ways to save the validity of the perturbation theory. Presumably the simplest possibility is to assume that the radiative corrections (2.7-2.9) arise not from one, but from several and possibly very many independent, or at most weakly coupled, scalar fields. In such a case the loop corrections from each independent field may be small, while their combined one-loop correction can add to a value close to unity. To illustrate the idea assume that that there are  $N \gg 1$  completely independent scalar fields  $\phi_i$  with equal cubic self-couplings living in the bulk. One would then have a truly small perturbation expansion parameter

$$\varepsilon_N \equiv \varepsilon/N \sim 1/N \quad (4.3)$$

for each separate field. In this case, the full perturbation expansions for the coefficients  $A, B$  and  $C$  appearing in the action (2.6) will be converging. Schematically for example:

$$A = \sum_{i=1}^N A_i = 1 + \#N\varepsilon_N + \#N\varepsilon_N^2 + \dots, \quad (4.4)$$

where  $\#$ s present numbers of order unity. If we now assume that the one-loop contribution is of order one, then the higher-loop corrections are suppressed by powers of  $1/N$ ; for example at two loops  $N\varepsilon_N^2 \sim \varepsilon/N \sim 1/N$ . Of course it is not necessary to assume that all fields have exactly the same couplings. It is enough that the sum of radiative corrections is chosen such that the combined one-loop contribution is of order one at present value of  $r$ . On the other hand, one must prevent large mixing couplings  $g_{ijk}$  in order to keep higher-loop corrections small. Indeed, at two loops in the strongly coupled limit one would find for example  $\delta A^{(2)} \sim N^2\varepsilon_N^2 \sim 1$ .

The same qualitative argument also apply to the function  $B$ . Tuning  $A$  close to zero does not imply that  $B$  is small at the same time however. Still, the neglected two-loop corrections are small for both quantities. The case of the Casimir potential is different however; for  $U$  there is no tree level contribution as the whole potential is purely of quantum origin. Its multi-field version corresponding to (4.4) then looks as follows:

$$U = \sum_{i=1}^N U_i = N U_N (1 + \# \varepsilon_N + \# \varepsilon_N^2 + \dots), \quad (4.5)$$

After we make the obvious identification  $N U_N = U_0 \sim 1$  we observe that the radiative correctios to  $U_0$  are truly small:  $c \sim \# \varepsilon_N \sim 1/N$ . This implies that the original ABRS-type stabilization relying on Casimir potential is not feasible in this construction.

## 4.2 New Radius Stabilization Mechanism

Fortunately, the simple perturbative scheme outlined above gives rise to a new radius stabiliation mechansim. Indeed, if the one-loop correction,  $\#N\varepsilon_N \equiv a \log(M_b r)$  in equation (4.4) is negative, then the function  $A(r)$  will become zero in the scale  $\log(M_b r_0) \simeq 1/|a|$ . The crucial observation is that now the two loop corrections to  $A, B$  and  $C$  are still small, so that the parametrization used in Eq. (2.6) remains valid. As a result, we can trust the

expression in Eqn. (3.5) for the Einstein frame potential  $V_E(\varphi)$  even when  $A \rightarrow 0$ .<sup>2</sup> The new radius stabilization now simply follows from the  $1/A^2$ -scaling of  $V_E(\varphi)$ , which makes it an increasing function of  $r$  as  $A$  approaches zero, and eventually gives rise to a narrow but infinitely high confining potential barrier at  $A = 0$ .

The potential shown in Fig. (1b) actually corresponds to  $A = 0$  confinement. The minimum seen there has nothing to do with the Casimir potential, for which we have in fact used a pure power law form with  $c = 0$ . Moreover, the sharp feature at the top of the potential maximum, the kink, corresponds to the singularity  $A(\chi_*) = 0$ , which would have shown up as an infinitely high and narrow spike in  $V_E(\varphi)$ . The fact that the singularity becomes a finite height kink in  $\chi$ -picture follows from the highly nontrivial relation between  $\chi$  and  $\varphi$  (see appendix A). One can understand this when one observes that also  $k^2(\varphi)$ -function becomes singular at  $A = 0$ , so that also the kinetic term for  $\varphi$  diverges. This has the opposite sign in the action and balances out the potential singularity. (Obviously the model should be qualified as a mixed  $k$ -essence and quintessence in the singular region.) Although  $V(\chi_*)$  is finite, note that it still is 20 orders of magnitude larger than the value of the potential at the minimum! Together with Hubble friction this barrier becomes a “brick wall”, that prohibits the field from reaching values beyond or even near  $\chi_*$  thus giving rise to a robust confinement mechanism to finite radii  $r < r_*$ .

In summary, we have shown that in a scenario with many weakly coupled independent fields the effective theory Eqn. (2.6) can be reliable even when  $A, B \approx 0$ . Large scale radius stabilization can not be obtained from Casimir potential because the scenario predicts  $C \approx 1$ , but it can originate from a singularity in the potential at  $A = 0$ . On technical side, the fact that the full one-loop contributions to quantities  $A$  and  $B$  are large, implies that one can not simplify any of the expressions that depend on them in the previous sections by expanding in  $a\varphi_0$  or  $b\varphi_0$  (one *can* expand  $C$ , or even put it to one, however), as was done in ref. [8]. This is of course the reason why we always kept the exact expressions.

## 5. Constraints

The underlying 6-dimensional model (2.6) has four unknown parameters:  $U_0$ ,  $a$ ,  $b$  and  $c$ . Given a full knowledge of the physics governing the six-dimensional world, these parameters could be calculated exactly in terms of the fundamental coupling constants, but as those details are not known, one has to settle with combinations of phenomenological and theoretical naturalness constraints. Radius stabilization arguments, together with the desired large values for  $r$ , have already settled the overall scale of the parameters  $U_0$ ,  $a$ ,  $b$  and  $c$ . We shall next impose the constraints coming from various observations.

### 5.1 Observational Constraints

There are four major observational constraints affecting the model parameters. We already

<sup>2</sup>We will see that unless  $N \gtrsim 1000$ , the cosmological evolution will tune  $A$  closer to zero than the scale of the two-loop corrections. This does not imply that we must include two-loop corrections to our results however. If we did, we would just find out that we have to tune the sum of one- and two loop results to a small value, but that the two-loop contribution remains much smaller than the one-loop term at all times, causing only minor changes to our results.

mentioned the gravity constraint in the previous section, and we shall return to it again shortly. Another constraint concerns the equation-of-state parameter for a dark energy component, which is limited by CMBR and astronomical data to [1]

$$w_\chi < -0.78. \quad (5.1)$$

To be precise, the limit (5.1) applies for the present value of  $w_\chi$ , and it was derived with the assumption that both  $w_\chi$  and  $\rho_\chi$  are constants. In the present model both the energy density and the pressure of the quintessence field are dynamical variables and so the bound (5.1) is not directly applicable. More general limits on function  $w_\chi(z)$  have been found in the literature [18]. However, parametrizations of the cosmic equation-of-state in terms of a pure dark energy  $w_\chi$  do not necessarily lead to an improvement over Eqn. (5.1). Indeed, imagine for example that the kinetic energy of a quintessence field is negligible so that  $w_\chi \sim -1$  to a high accuracy over the range of interest in  $z$ . The predictions of the model can still differ significantly from a pure cosmological constant if  $V(\chi(z))$  continues to evolve in the scale  $\rho_c$  (giving rise to a variable total  $w(z)$ ). This actually will be precisely the case in the examples presented below. However, we take Eqn. (5.1) as an indication that the present value of  $w_\chi$  should be very close to  $-1$ . It is convenient to rephrase Eqn. (5.1) in terms of present ratio of the kinetic and the potential energy densities of the  $\chi$ -field:

$$\delta_\chi \equiv \frac{1+w_\chi}{1-w_\chi} < 0.12. \quad (5.2)$$

Third observational constraint comes from connecting the model parameters with the present observational value of the dark energy density:

$$V(\chi_0) \equiv M_b^4 U_0 \frac{1}{(M_b r_0)^8} \frac{C_0}{A_0^2} = \frac{\Omega_\Lambda \rho_c}{1 + \delta_\chi}, \quad (5.3)$$

where  $\Omega_\Lambda \approx 0.73$ . The content of Eqn. (5.3) is that a given set of model parameters  $U_0$ ,  $a$  and  $c$ , and the boundary condition for  $\delta_\chi$  will determine the precise value of  $M_b r$  today. Because  $\rho_c \sim 10^{-120} M_b^4$  in natural units, it is clear that setting  $U_0 \sim 1$ , imposes roughly the desired scale of  $M_b r \sim 10^{15}$ .

Finally, there is a constraint due to the need of preserving the success of big bang nucleosynthesis. This has at least the following two implications: First, the universe must be radiation dominated already at BBN-time. This constrains both the kinetic and potential energy densities of the scalar field, which would otherwise make the universe expand too fast and result in too large helium production. Second, the weak interaction rates controlling the proton-to-neutron ratio, and eventually of the abundances of the light elements produced, are proportional to particle masses (proton and  $W$ -masses to be precise). Since the masses scale as  $\propto 1/M_b r \sqrt{A}$  in our model, this implies that  $M_b r$  must remain approximately constant between now and BBN-scale. These considerations do not lead to additional constraints on model parameters, but rather to a need for tuning the initial conditions for the quintessence field. There is a correlation between the two however, because different sets of model parameters need different sets of initial conditions to provide

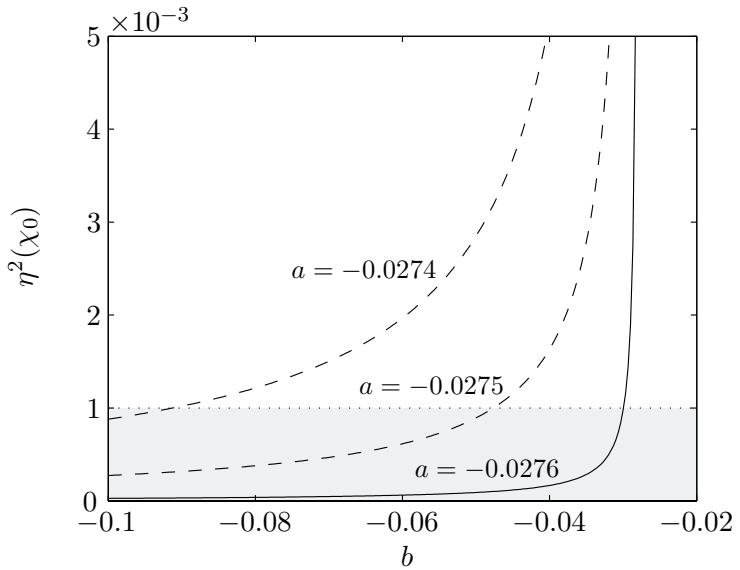


**Figure 2:** Shown is the present value of the square of the  $\eta$ -coefficient as a function of the parameter  $b$  for three different values of the parameter  $a$ . The other model parameters are set to the values given in Eqn. (5.4). The region below the dotted line is allowed by the constraint (4.2).

an acceptable cosmological solution. Moreover, it is not *a priori* clear that acceptable solutions do exist at all for arbitrary sets of model parameters, and eventually, even if solutions fulfilling present day constraints are found, one has to check that the corresponding initial conditions are natural in the model building sense. All these questions can only be studied through numerical analysis.

## 5.2 Fine-Tuning in the Model Parameter Space

Let us once again consider the gravity constraint Eqn. (4.2) ( $\eta$ -bound for short). While the form of the potential automatically adjusts  $A$  close to zero, it is not immediately clear whether this tuning is sufficient to satisfy the  $\eta$ -bound automatically. Comparing Eqns. (4.2) and (3.10) we see that there is in fact some tension between fulfilling the  $\eta$ -bound and reaching the potential minimum where  $V'(\chi) = 0$ . Indeed, for  $c = 0$  the latter corresponds to  $A = -a/4$ , whereas the former goes to zero at  $A = -a/2$ . Whether this difference can be accommodated obviously depends on how strict the eta-constraint really is. From the parametric dependence of  $\eta = \eta(M_b r_0, a, b)$  (cf. Eqn. (3.11)) one sees that the  $\eta$ -bound leads to correlations between the model parameters, and so does the need to adjust  $V$  to the present cosmological constant as well. In the end one is forced to some cross-correlated fine-tuning with the model parameters. Instead of trying to map out the allowed region in the parameter space, we estimate the degree of the fine-tuning that is needed by fixing all other parameters to some natural values and then checking how much freedom is left in varying  $a$ . Observe that this does not mean that  $a$  is *a priori* the parameter to be fine tuned; we could as well fix  $a$  rather freely, and then fine-tune either  $U_0$ , or even the radius of the extra dimensions today  $r_0$ .

Let us assume that  $M_b r_0$  is fixed. For definiteness we assume that the potential and  $\delta_\chi$  parameters take on the values

$$U_0 = 2.68, \quad c = 0 \quad \text{and} \quad \delta_\chi = 10^{-2}. \quad (5.4)$$

For a fixed  $M_b r$  the  $\eta$ -bound implies that  $A + a/2$  has to be fine-tuned to zero to an accuracy

$$|A + a/2| \leq \sqrt{a\eta_0^2|B|}. \quad (5.5)$$

Because of the smallness of  $\eta_0^2$  this is always rather strong constraint, and it becomes particularly severe when  $|B|$  is small. This dependence is clearly visible in Fig. (2), where we plot  $\eta$  as a function of  $b$  for some representative values of  $a$ . For the values chosen above,  $|B|$  goes to zero at  $b_* \approx -0.0279$ ,<sup>3</sup> and the closer  $b$  gets to  $b_*$  the more accurately  $a$  must be fine tuned to a value  $a \rightarrow b_*/(1 - b_*/2) \approx -0.0276$ . If we now impose the perturbative argument that  $|b|$  is of the same order as  $|a|$ , it implies that  $a$  has to be fine-tuned to roughly one part in ten thousand, which corresponds to a relative accuracy of about one per cent. This gives an estimate of the amount of fine-tuning that is needed when adjusting different acceptable model parameter sets. In what follows we shall fix  $a$  to the value that allows the widest interval in  $b$  in Fig. (2), *i.e.*

$$a = -0.0276 \quad \text{and} \quad b < -0.0300. \quad (5.6)$$

Equations (5.4, 5.6) define the allowed parameter space for our quintessence-like scenarios with two large extra dimensions. Changing  $U_0$  and  $c$  only moves solutions to a slightly different band in  $a$  and  $b$  space. To be specific, we will choose  $b = -0.031$  as our reference value in what follows.

Finally note that the expression on the right-hand side of equation in general is smaller than  $a/4 \approx 0.007$ . Indeed, for our reference value of  $b$  we have  $\sqrt{a\eta_0^2|B|} \approx 0.0014$ . As a result the cosmological evolution must be such that the field is actually *not* in its minimum at present. Moreover, all our solutions should show some late time evolution and adjustment of  $\eta$  close to the present time. One can lessen this effect by choosing a large value for  $|B|$ , but apart from such additional tuning the late evolution should be a generic prediction of the model.

### 5.3 Phantom Parametrizations

For our reference set Eqns. (5.4-5.6), the model stays non-phantom for all values of  $r$ , also beyond the  $A = 0$  singularity where normal matter would be tachyonic. For more negative values of  $b$  the field  $\varphi$  becomes phantom over a finite  $r$ -interval in the tachyonic phase as shown in Fig. (3a). But since the field evolution never enters the tachyonic phase, these phantom-tachyonic cosmologies cannot be realized from natural initial conditions. However, it is also possible to arrange the model parameters such that  $\varphi$  becomes a phantom field already before the  $A = 0$  singularity. We show examples of such models in Fig. (3b).

---

<sup>3</sup>One can find through Eqns. (5.3) and (5.4), together with the *a posteriori* knowledge that  $a$  is almost fixed, that  $M_b r_0 \approx 3.46 \times 10^{15}$  and then  $b_* = 1/\log(M_b r_0) \approx -0 - 0279$ .

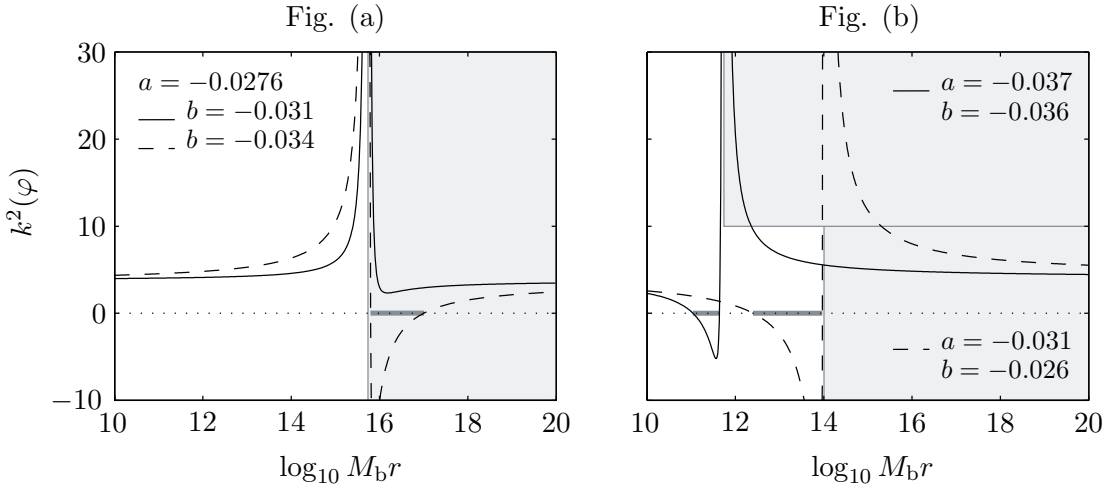


**Figure 3:**  $k^2(\varphi)$  as a function of  $\log_{10} M_{\text{br}} r$  ( $= \varphi / \log 10$ ) for different values of the parameters  $a$  and  $b$ . Thick gray lines highlight the values of the radius that correspond to phantom phase in  $\chi$ . Shaded regions correspond to the values where ordinary matter would become tachyonic.

It is quite interesting that these phantom-like structures were found using perfectly natural values of model parameters. Nevertheless, it is not clear to us whether one can arrange a phantom phase into the past, present or the future of *our* universe such that it would be compatible with all the observational constraints. At least the examples that we have studied, including the models shown in Fig. (3b) almost certainly are ruled out by gravity constraints. However, it could be that by loosening the fundamental restrictions on the model, such as the millimeter scale for extra dimensions, one could obtain a richer structure of possibly acceptable mixed phantom-quintessence- $k$ -essence solutions.

#### 5.4 Other Constraints

Some of the constraints discussed so far were generic to any effective quintessence model. Others, such as the need for the large scale radius stabilization, were particular to the present model having its origin in large extra dimensions. There is yet another type of constraint particular to models with large extra dimensions that we need to discuss. Namely, the radion degree of freedom that we have seen to give rise to quintessence field, comes associated with an infinite tower of Kaluza-Klein excitations on the brane. The problem with the KK-modes is that if the universe enters the radiation dominance at too high temperature  $T_*$ , too many KK modes might be excited through their couplings with ordinary particles [20–22]. However, it is quite difficult to state precisely how these considerations limit the model parameters, because they depend on introducing an entire new structure to the model, which has not yet been explored in detail. Indeed, the problem of KK-modes might be associated and solved by the unknown higher-dimensional physics, in which case even no additional constraints might arise [8]. Even in the more conservative view, which assumes the possibility of exciting the KK-modes at the reheating scale  $T_*$ , bounds depend on the details of the temperature history on the brane. They can be quite stringent however;

for example, Hannestad [22] reports that if the universe enters radiation dominace instantly, then the fundamental mass scale (having fixed  $M_b r$ ) is bounded by  $M_b \gtrsim 8 + 10(T_*/\text{MeV})$  TeV. In principle we can always accommodate such a constraint in our model. This would of course to some degree undermine the particle physics motivated attraction to it, which originates from connecting the fundamental gravity and weak scales to evade the heirarchy problem. From a cosmology point of view, the main problem is however that an increase in  $M_b$  must be compensated by a decrease in  $r$ , which would eventually spoil the naturalness of the Casimir potential as the source of dark energy. The situation is not extreme however; taking a reheating temperature  $T_* = 1$  MeV, gives  $r \lesssim (0.02\text{eV})^{-1}$ , which would still imply a reasonably modest fine-tuning of order  $U_0 \sim 10^{-5}$ .

## 6. A Realistic cosmology

In the previous section we showed that setting the fundamental energy scale to TeV, or equivalently, the stabilized extra dimensions to millimeter scale, combined with theoretical and observational constraints practically fixes the fundamental parameters in the model. This means that the form of the quintessence potential  $V(\chi)$  is almost set as well, not leaving much extra space for adjustments to get an acceptable cosmological evolution. Of course, a lot has already been achieved in the course of fixing the parameters; built in is the feature that the potential has a minimum corresponding to millimeter scale such that  $V(\chi)$  would give the right amount of dark energy today. Also, the gravity constraints and constraints on the equation-of-state parameter are automatically satisfied if the field sits near the potential minimum. However, we still have to show that model can support a cosmological evolution consistent with all constraints, leading to the desired densities at present.

Let us stress that we actually do not know the full theory at the fundamental TeV-scale; we have to our disposal only an effective theory that is valid at much lower energy scales. In fact, the thermal history beyond the entrance to radiation dominance is subject to unknown physics related to the Kaluza-Klein excitations and the constraints arising thereof [20–22]. We will therefore start off the evolution of our model universe at a temperature well below the TeV-scale,  $T \ll 1$  TeV, but still above the big bang nucleosynthesis temperature of  $T \sim 1$  MeV. In practice we are using the scale factor  $R$  as an integration variable; setting  $R_{\text{now}} \equiv 1$  we have  $R_{\text{BBN}} \approx 10^{-10} - 10^{-9}$ , and  $R_{\text{TeV}} \approx 10^{-16}$ . Having chosen a suitable starting point  $R_{\text{start}}$ , we integrate the evolution equations until present with variable initial conditions for  $\chi$  and  $\dot{\chi}$  until (if) an acceptable solution is found.

We now turn to the qualitative features to be met by an acceptable solution. First one has to make sure that the model doesn't spoil the BBN explanation for the observed light element abundances. As was explained in the previous section, this is ensured if  $M_b r$  was already very close to its present value during BBN. This turns out to be a tough constraint, which basically forces us to set the field relatively close to its potential minimum at  $R_{\text{start}}$ . Fixing BBN combined with the constraints built into our model potential, go a long way towards fixing the correct cosmological model today. What remains is essentially the issue of getting the quantitative values of present energy densities  $\Omega_\chi \approx 0.73$  and  $\Omega_m \approx 0.27$

Variable	Starting Value	Present Value
$\tilde{\chi}$	-20.2	-12.4
$\partial\tilde{\chi}/\partial\tilde{t}$	$2.1 \times 10^{-37}$	$3.23 \times 10^{-61}$
$\log_{10} M_{\text{br}}$	14.2	15.5
$\tilde{\rho}_\chi$	$2.2 \times 10^{-74}$	$8.44 \times 10^{-121}$
$\tilde{\rho}_m$	$2.1 \times 10^{-84}$	$3.18 \times 10^{-121}$
$\tilde{\rho}_r$	$2.9 \times 10^{-76}$	$2.90 \times 10^{-124}$
$\log_{10} R$	-12.0	0.00
$\tilde{\rho}_{\text{tot}}$	-	$1.16 \times 10^{-120}$
$\Omega_\chi$	-	0.726
$\Omega_m$	-	0.274
$\Omega_r$	-	$2.49 \times 10^{-4}$
$w_\chi$	-	-0.876

**Table 1:** Initial conditions/starting values and the resulting values at present. Quantities with a tilde are given in units of  $M_b$ , *i.e.*  $\tilde{\chi} \equiv \chi/M_b$ ,  $\tilde{t} \equiv M_b t$ , and  $\tilde{\rho} \equiv \rho/M_b^4$ . Note that  $\tilde{\rho}_{\text{tot}} = 1.16 \times 10^{-120} = \tilde{\rho}_c$ .

to coincide with  $\rho_{\text{tot}} \approx \rho_c$ . This of course is just the familiar “why now” problem, which in general requires some fine-tuning of initial conditions in generic quintessence models. Here the “why now” problem is essentially transformed to the assumed millimeter scale of extra dimensions. Below we present an example of a realistic cosmology corresponding to our basis set of model parameters;  $U_0 = 2.68$ ,  $a = -0.0276$ ,  $b = -0.031$  and  $c = 0$ . We have started the evolution at the scale  $R_{\text{start}} = 10^{-12}$ , which roughly corresponds to  $T_{\text{start}} \simeq 100$  MeV. The corresponding initial conditions/present values of  $\chi$ ,  $\dot{\chi}$  etc. are given in Table 1, and the cosmological evolution of energy densities,  $\rho_i$ , the radius  $M_{\text{br}}$ , the coupling function  $\eta$  and the equation-of-state parameter  $w_\chi$  are shown in Figs. (4, 5a, 5b, and 6) respectively. Note that we have extended the evolution a bit further than present, with grey areas representing the future.

Due to the large starting value of  $M_{\text{br}}$ , the potential is negligible compared to the kinetic energy and the scalar field enters radiation domination in a kinetic-dominated roll. During early stages, the kinetic energy scales as  $\dot{\chi}^2 \propto R^{-6}$ , and it dominates the energy density for  $R \lesssim 10^{-11}$ . This scaling follows from (3.9) when the potential and the  $\eta$ -terms are neglected and the evolution of the scalar field is dominated by the Hubble friction  $3H\dot{\chi}$ . During this *kination* phase [19] the field  $\chi$  is rolling down its potential and the radius of the extra dimensions is growing rapidly. The scalar field dominance ends and the universe enters radiation domination right before BBN. At this time  $\chi$  settles close to the minimum of the potential (see Fig. (1b)), and correspondingly the radius reaches a plateau as shown in Fig. (5a). The energy of the scalar field continues to fall rapidly, until kination is halted by the  $\eta$ -term. The  $\eta$ -term causes  $\dot{\chi}^2$  to track matter density until  $\log_{10} R \approx -1.5$  (redshift  $z \approx 30$ ), where the kinetic energy falls below the potential, and the  $\chi$ -field starts acting like a cosmological constant.

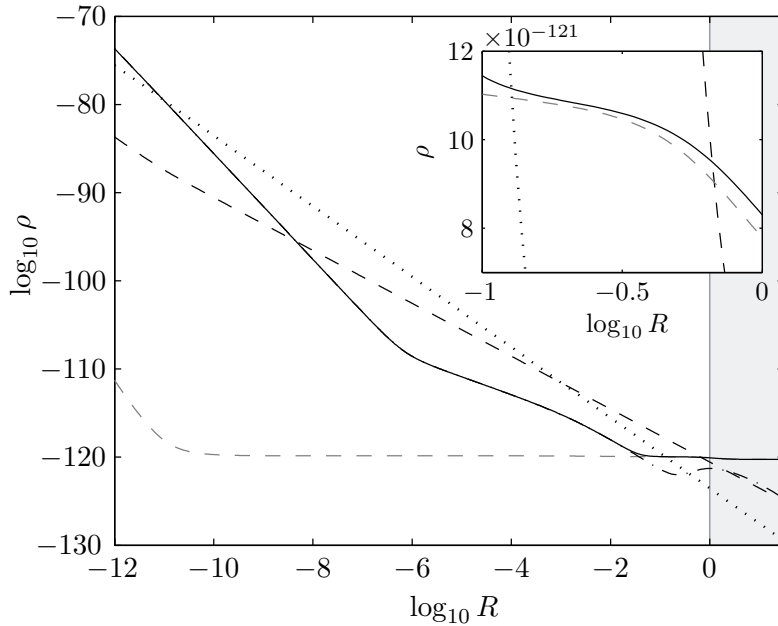


**Figure 4:** Different components of the energy density (in Planck units) as a function of the scale factor  $R$ . The various curves represent matter (dashed black), radiation (dotted) and scalar energy density (solid). The dashed grey and dot-dashed curves shows potential and kinetic part of the scalar energy density, respectively. The scale factor is normalized to one at present.

Although  $V(\chi)$  now dominates the total energy density, it is not yet a constant (see the linear scale plot inserted in Fig. (4)). The cause for this final 20% decrease between  $z \approx 0.5$  and present can be tracked to the tension between the  $\eta$ -constraint and the position of the potential minimum for our model parameters, discussed in section (5.2). Indeed, for a long time, the  $\eta$ -term acts like an additional effective potential in the equation of motion (3.9) and confines the field to the proximity of the zero of the  $\eta$ -function at  $A \sim -a/2$ .<sup>4</sup> As the matter density becomes very small, the  $\eta$ -term eventually becomes small in comparison to the potential gradient, and the field can finally roll down to its true minimum. This phase can also be seen as a slight increase in  $M_{\text{br}}$  in Fig. (5a), as well as in a little more dramatic change  $k^2(\varphi)$  and in the  $\eta$ -function itself shown in Fig. (5b). For the particular solution we have displayed in detail, the  $\eta$ -constraint is in fact barely satisfied at present. Our discussion in section (5.2) suggests that we can do better by using a somewhat larger value for  $b$ , because this allows more flexibility in  $\eta$ -limit. We can see that this reasoning works from Fig (5b), which also shows an  $\eta$ -evolution corresponding to  $b = -0.034$ , while other parameters are kept to our reference values. For very large  $b$  the tension actually vanishes and one should obtain acceptable solutions even when reaching the true minimum of the potential. For a large part of the parameter space, the temporary dominance of the effective  $\eta$ -potential is a necessary prerequisite for an acceptable solution however.

The evolution of both  $w_\chi$  and  $w_{\text{tot}}$  are shown in Fig. (6). The epochs of kination ( $w_{\text{tot}} = 1$ ), radiation dominance ( $w_{\text{tot}} = 1/3$ ), matter dominance ( $w_{\text{tot}} \approx 0$ ) and the eventual

<sup>4</sup>This behaviour of the  $\eta$ -term has been discovered elsewhere in the context of chameleon models [23].

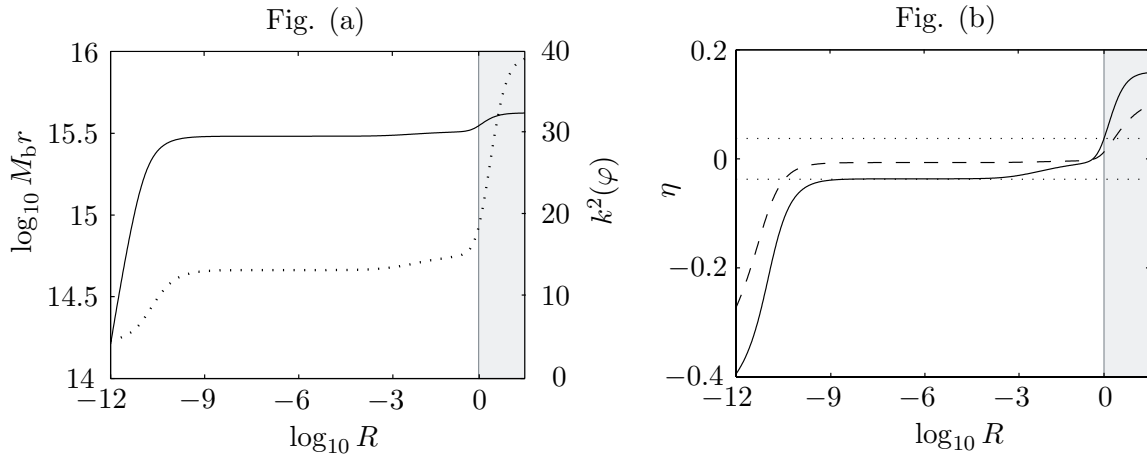


**Figure 5:** (a) Shown is  $\log_{10} M_b r = \varphi / \log 10$  (solid line) and the  $k^2(\varphi)$ -factor defined in Eqn. (3.6) (dotted line) as a function of the scale factor  $R$ . (b) The coupling  $\eta$  as a function of the scale factor  $R$  for two different set of parameters: solid line corresponds to the set given in the text and the dashed line to another solution with  $U_0 = 2.46$ ,  $a = -0.0276$ ,  $b = -0.034$ , and  $c = 0$ .

cosmological constant dominance when  $w_{\text{tot}} \rightarrow -1$  are clearly visible. The evolution of  $w_\chi$  is much less dramatic. It remains close to unity all the way until  $\log_{10} R \approx -2$ , when it rapidly falls from  $w_\chi = 1$  to close to  $w_\chi = -1$ , as the kinetic energy of the field becomes negligible in comparison to the potential energy. The only interesting feature is the little bump in  $w_\chi$  which is caused by the small temporary increase in the kinetic energy of  $\rho_\chi$ , as  $\chi$  makes its last roll closer to the potential minimum.

In summary, it is clear from Fig. (4) and Table 1 that the evolution of all densities have the desired features. In particular, the universe is flat with  $\Omega_\chi = 0.73$  at present. Also, as shown in Figs. (5a) and (5b), both  $M_b r$  and  $\eta$  fulfill the observational constraints. Overall, the evolution of the energy densities is qualitatively surprisingly similar to the results of Albrecht *et al.* [8], apart from the additional evolution at late times, that we have seen to be connected with the mismatch between the zero of the  $\eta$ -function (3.11) and the minimum of the potential  $V(\chi)$ .

### 6.1 Quintessence Vs. $\Lambda$ -Cosmology

Although the scalar field behaves like a cosmological constant at present, it obviously had a varying equation of state in the past. This allows for a possibility to put bounds on the model based on observations that can probe the equation of state at different times. We have therefore computed the magnitude-redshift relation of type Ia supernovae, predicted by our reference case. This relation will be measured to high accuracy by the SNAP-satellite [11] in the near future. The results are given in Fig. (7a), where the redshift-magnitude diagram is shown normalized to a corresponding flat,  $\Omega_\Lambda = 0.73$  cosmology. Comparing with the shown binned simulated SNAP data obtained from ref. [12], suggests that the satellite experiment should easily be able to distinguish the models from each other. This interpretation is verified by Fig. (7b), which shows a  $\chi^2(\sigma_i)$  function in the space of

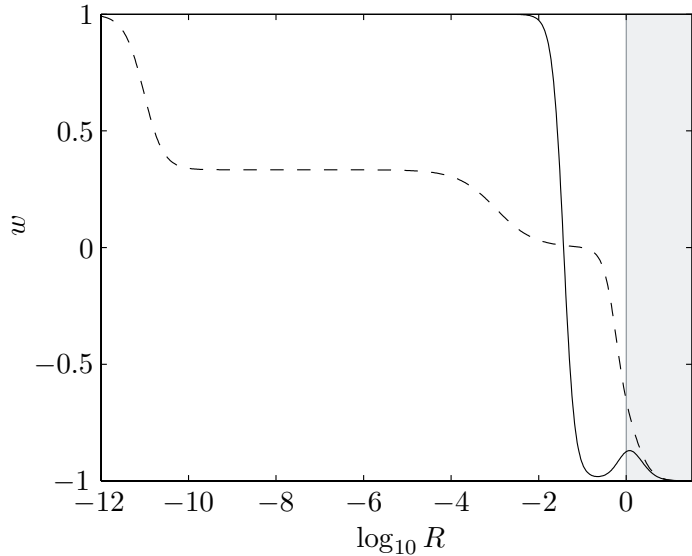


**Figure 6:** The equation-of-state parameters  $w_\chi$  (solid) and  $w_{\text{tot}}$  (dashed) as functions of the scale factor  $R$ .

constant  $\Lambda$  models using our quintessence scenario with  $\Omega_{\chi_0} = 0.73$  as null hypothesis. The  $\Omega_\Lambda = 0.73$  model lies clearly several sigmas away from the present model. However, the minimum of the  $\chi^2$ -function at  $\Omega_\Lambda = 0.69$  lies well within one sigma from the null hypothesis. Thus, SNAP data alone will not be able to distinguish between our model and the  $\Lambda$  models with about 5 % less dark energy. While the difference is small, it might be possible to break the degeneracy by combining SNAP-data with current data on the cosmic microwave background anisotropies.

Let us briefly return to analyze the difference between the present model and the  $\Lambda$ -cosmology in the magnitude-redshift relation: Can one infer this difference from the plot for  $w_\chi$ , which shows the peculiar bump right in the region of interest for supernova observations? The answer turns out to be negative; one could essentially discard the evolution of  $w_\chi$  (that is put  $\dot{\chi}^2$  to zero at  $z < 1$ ), and yet obtain the same result. The fact that  $w_\chi \approx -1$  below  $z \sim 1$ , arises simply because the kinetic energy of the  $\chi$ -field is negligible compared to the potential, but it does not imply that the model is equivalent with a constant  $\Lambda$  model in this region. Indeed, it is clearly visible from Fig. (6) that the potential still falls by 20% between  $z \approx 1$  and now, and because the universe is potential dominated during this period, the true cosmic equation of state is necessarily quite different from a constant  $\Lambda$  model.

What one should learn from this is that it can be quite impractical to try to put bounds on models based solely on the information on  $w_\chi(z)$ . This reduces the applicability of some recent bounds based on different phenomenological parametrizations of the  $w_\chi(z)$ -function [22, 24]. Instead, the relevant quantity for the observation, and the one that should be modelled, is the full equation-of-state parameter  $w_{\text{tot}}(z)$ . Let us finally remind that the late time evolution in the potential is a rather generic feature of the present model,

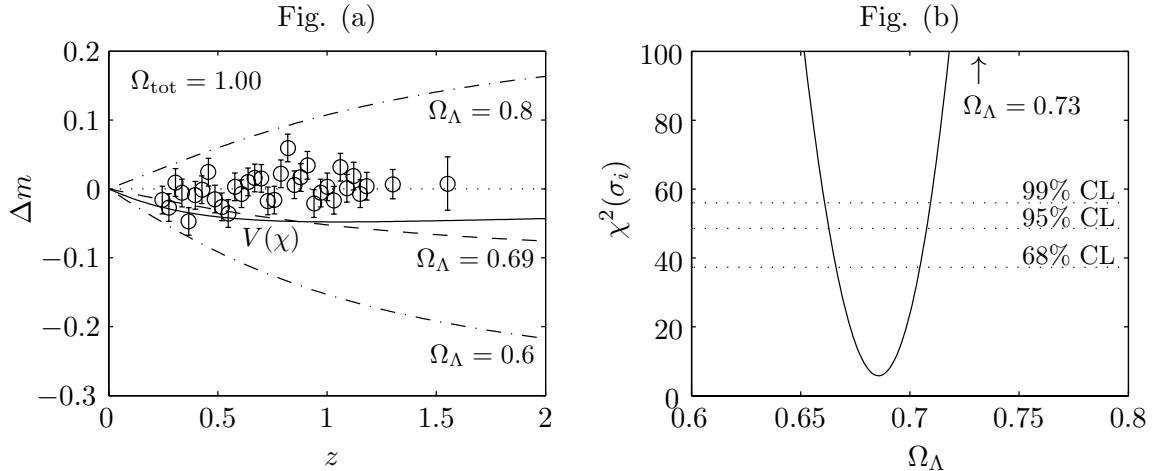


**Figure 7:** (a) Redshift-magnitude diagram normalized to a flat,  $\Omega_{\Lambda} = 0.73$  cosmology, with binned simulated SNAP data [12]. The solid line representing the quintessence scenario corresponds to  $\Omega_{\chi} = 0.73$  at present. (b) Statistical  $\chi^2(\sigma_i)$  for a cosmological constant, using the quintessence scenario with  $\Omega_{\chi} = 0.73$  at present as null hypothesis.

and therefore so is the observed difference in the magnitude-redshift relation between the present model and a corresponding constant  $\Lambda$  model.

## 6.2 Robustness of the Radius Stabilization

Let us finally consider the robustness of the radius stabilization mechanism based on the  $A = 0$  singularity. On one hand, the potential barrier looks ridiculously small, when compared to the potential at very high scales. On the other hand, as mentioned above, the barrier height is about 20 orders of magnitude higher than the value of the potential at the minimum. Could it nevertheless be possible to go past the barrier and make the world enter the tachyonic phase, by giving the field a much larger initial velocity? The answer turns out not to be the case; no matter how large an initial velocity we give the field, the solution always either gets stuck close to the singularity, or starts oscillating back and forth until its kinetic energy energy gets diluted by the Hubble friction. We show an example of such an evolution in Figs. (8a-8b), where we have used the same model parameters and the initial conditions as shown in the Table 1, apart from having given the field 12 orders of magnitude larger kinetic energy. Now the potential reaches its minimum already at  $\log_{10} R \approx -11$  and starts increasing again as the field continues climbing the potential barrier (see Fig. (1b)). The growth of  $\chi$  and therefore also that of  $r$  stops at  $\log_{10} R \approx -6$ , where the potential energy reaches its maximum and the kinetic energy goes through zero (this shows as a small dip in Fig. (8a)). The huge spike in the  $k^2(\varphi)$ -function shows that the field came close to the singularity before turning back. As the field rolls back,  $r$  is changing slowly initially, because of the near singular relation between  $\chi$  and  $r$ , but eventually at about  $\log_{10} R \approx 3$  (far in the future)  $r$  makes a small adjustment back before freezing out completely as the universe finally reaches De Sitter character. After

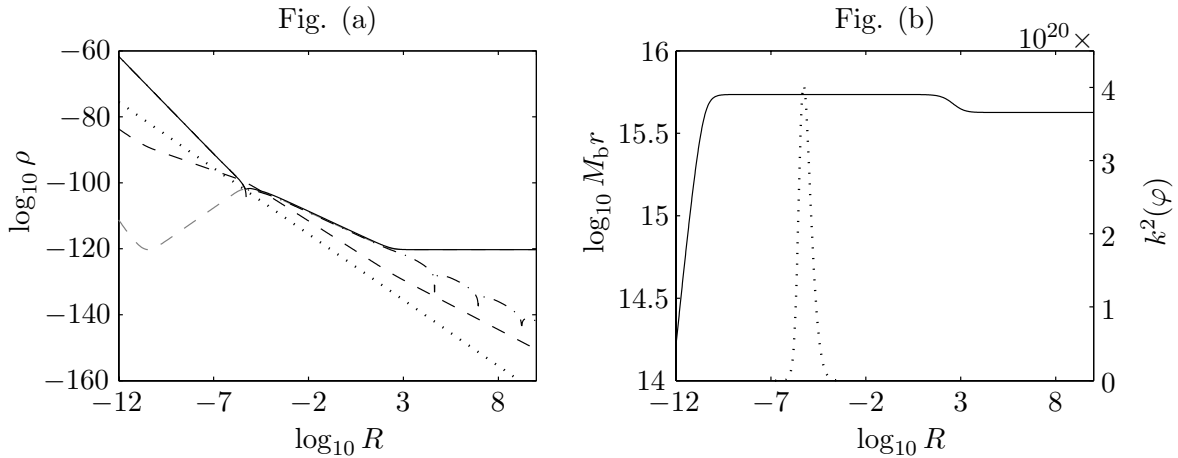


**Figure 8:** (a) Shown are energy densities as a function of the scale factor  $R$  for the same model parameters and initial conditions as in Fig. (4), except for the field velocity, which here is  $\partial\tilde{\chi}/\partial\tilde{t} = 2.1 \times 10^{-31}$ . Different curves represent matter (dashed black), radiation (dotted), total scalar energy density (solid), scalar potential energy (grey dashed) and scalar kinetic energy (dot-dashed). (b) Shown is  $\log_{10} M_b r = \varphi / \log 10$  (solid line) and the  $k^2(\varphi)$ -factor defined in Eqn. (3.6) (dotted line) as a function of the scale factor  $R$ .

this the field rolls a few times back and forth over the minimum during De Sitter phase as the Hubble friction absorbs the remaining kinetic energy. Observe that most of the time during the period of backwards rolling the universe is neither matter, radiation, or cosmological constant dominated, nor does it behave like during  $\dot{\chi}^2$ -dominated kination. Instead, it is a peculiar mix of kinetic ( $k$ -essence) and potential (quintessence) energy. Needless to say, this example is entirely incompatible with our universe; we only gave it to show the robustness of the radius stabilization against initial conditions with very large field velocities.

## 7. Summary and Discussion

We have considered in detail a large extra dimension inspired model for the cosmic dark energy, based on ideas put forward by Albrecht et al. [7, 8]. In this model the effective quintessence field  $\chi$  corresponds to a radion mode originating from dimensional reduction of a full 6D action to an effective 4D brane action. We have shown that observational gravity constraints ( $\eta$ -parameter) necessitate a somewhat novel realization of the 6D scalar field configuration, where the radiative one-loop corrections from scalars nearly cancel tree level contribution to the effective 4D Ricci scalar at present. This cancellation shows up as a singularity in the conformal transformation between Jordan and Einstein metrics and gives rise to a new type of large-radius stabilization, which moreover makes model automatically almost consistent with the  $\eta$ -constraint. A by-product of the new perturbative scheme is that the corrections to the lowest order Casimir potential are truly small, and can no more give rise to a radius stabilization, as was assumed in the original work [8]. However, the

“new” radius stabilization relies on the same physical principles as did the “old” one: the renormalizability of the scalar field interactions in 6D.

We have shown that depending on the parameters, the model can give rise to features very different from a generic quintessence model. To a degree this was already recognized by the earlier work, and indeed the model has been dubbed “walking quintessence” [9]. However, we have shown that the model can behave at times more like a  $k$ -essence, where the dynamics is mainly controlled by the kinetic term, or even as a phantom cosmology, where the kinetic term of the effective radion field changes sign. Typically the phantom phases have a finite range in  $r$ , allowing for the possibility of a finite duration phantom phase, possibly side-stepping the associated problems of vacuum instability in such models [13]. It would be interesting to see if such phantom realizations could be made consistent with the observations. Moreover, we pointed out the (even more) academic, but curious feature that beyond the confining singularity all normal matter would become tachyonic.

We then showed that imposing various constraints very nearly determine all the fundamental parameters in the effective 4D brane action. Moreover, some of the parameters or combinations of parameters needs to be fine tuned to a rather high degree for the model to work. (That is, to simultaneously give rise to a large enough radius consistent with the gravity constraint.) Nevertheless, having fixed the parameters, we show that the model can give rise to an acceptable cosmological evolution. Moreover, the model predicts a characteristic signature in the magnitude-redshift relation of type Ia supernovae, that may make it possible for a combination of supernova and CMBR data to distinguish the model from a pure  $\Lambda$ -cosmology.

A particularly attractive feature of the present model is that it makes a clear identification for the origin of the effective quintessence field in a well defined model that has a motivation beyond cosmology. Indeed, models with large extra dimensions were originally proposed as a novel solution to the hierarchy problem [20, 25]. This blessing comes with a burden however. We have seen that cosmology puts several stringent constraints on the model parameters and leaves little freedom in choosing the initial conditions of the cosmological evolution. A particularly ugly feature is that one is forced to assume a very large value for the radius  $r$  as the universe enters the radiation dominance. Moreover, the thermal history of the model is heavily constrained by the need to avoid overproducing Kaluza-Klein modes. This depends on various assumptions on the reheating phase, and as these features are not included in the present treatment, little can be said about the evolution of the universe above a few MeV. In this respect our present model does no better nor worse than the original work [7, 8], and we refer the reader there for more discussion on this issue.

Another limitation of the current treatment concerns the phenomenological parametrization (2.6-2.9) for the 4D action. Since we are finding that the log-terms need to be large, it would be better to use some renormalization group improved expressions for the coupling functions instead. We do not believe that this is more than a qualitative problem however, since for the confinement and for satisfying the  $\eta$ -constraint it is basically enough that the function  $A$  is monotonically decreasing and has a zero at a logarithmically large scale in  $r$ . It would be interesting to study this question in more detail however, also from the

point of view of computing the parameters  $a, b, c$  and  $U_0$  from a definite realization of the underlying 6D model. This task is beyond the scope of the present paper however.

## Acknowledgements

We would like to thank Edward Mörtsell for useful discussions on supernovae constraints. This work was partially supported by the CIMO-grant TM-04-2500.

## References

- [1] D. N. Spergel *et al.*, *First Year Wilkinson Microwave Anisotropy Probe (WMAP) Observations: Determination of Cosmological Parameters*, *Astrophys. J. Suppl.* **148** (2003) 175 [arXiv:astro-ph/0302209].
- [2] P. J. E. Peebles and B. Ratra, *Cosmology With A Time Variable Cosmological 'Constant'*, *Astrophys. J.* **325** (1988) L17.
- [3] B. Ratra and P. J. E. Peebles, *Cosmological Consequences Of A Rolling Homogeneous Scalar Field*, *Phys. Rev. D* **37** (1988) 3406.
- [4] C. Wetterich, *Cosmologies With Variable Newton's 'Constant'*, *Nucl. Phys. B* **302** (1988) 645.
- [5] J. J. Halliwell, *Scalar Fields In Cosmology With An Exponential Potential*, *Phys. Lett. B* **185** (1987) 341;  
P. G. Ferreira and M. Joyce, *Structure formation with a self-tuning scalar field*, *Phys. Rev. Lett.* **79** (1997) 4740 [arXiv:astro-ph/9707286];  
E. J. Copeland, A. R. Liddle and D. Wands, *Exponential potentials and cosmological scaling solutions*, *Phys. Rev. D* **57** (1998) 4686 [arXiv:gr-qc/9711068];  
P. G. Ferreira and M. Joyce, *Cosmology with a Primordial Scaling Field*, *Phys. Rev. D* **58** (1998) 023503 [arXiv:astro-ph/9711102];  
T. Barreiro, B. de Carlos and E. J. Copeland, *Stabilizing the dilaton in superstring cosmology*, *Phys. Rev. D* **58** (1998) 083513 [arXiv:hep-th/9805005];  
T. Barreiro, E. J. Copeland and N. J. Nunes, *Quintessence arising from exponential potentials*, *Phys. Rev. D* **61** (2000) 127301 [arXiv:astro-ph/9910214].
- [6] A. Albrecht and C. Skordis, *Phenomenology of a realistic accelerating universe using only* *Phys. Rev. Lett.* **84** (2000) 2076 [arXiv:astro-ph/9908085].
- [7] A. Albrecht, C. P. Burgess, F. Ravndal and C. Skordis, *Exponentially large extra dimensions*, *Phys. Rev. D* **65** (2002) 123506 [arXiv:hep-th/0105261].
- [8] A. Albrecht, C. P. Burgess, F. Ravndal and C. Skordis, *Natural quintessence and large extra dimensions*, *Phys. Rev. D* **65** (2002) 123507 [arXiv:astro-ph/0107573].
- [9] C. P. Burgess, *Natural quintessence and the brane world*, [arXiv:astro-ph/0207174].
- [10] T. Damour and K. Nordtvedt, *Tensor - scalar cosmological models and their relaxation toward general relativity*, *Phys. Rev. D* **48** (1993) 3436.
- [11] SNAP: <http://snap.lbl.gov>.
- [12] J. Weller and A. Albrecht, *Opportunities for future supernova studies of cosmic acceleration*, *Phys. Rev. Lett.* **86** (2001) 1939 [arXiv:astro-ph/0008314].

- [13] R. R. Caldwell, *A Phantom Menace?*, *Phys. Lett. B* **545** (2002) 23 [arXiv:astro-ph/9908168].  
S. M. Carroll, M. Hoffman and M. Trodden, *Can the dark energy equation-of-state parameter w be less than -1?*, *Phys. Rev. D* **68** (2003) 023509 [arXiv:astro-ph/0301273].
- [14] J. Weller, *Bubbles from dark energy?*, arXiv:astro-ph/0004096.
- [15] R. R. Caldwell, R. Dave and P. J. Steinhardt, *Cosmological Imprint of an Energy Component with General Equation-of-State*, *Phys. Rev. Lett.* **80**, 1582 (1998) [arXiv:astro-ph/9708069].
- [16] A. Hebecker and C. Wetterich, *Natural quintessence?*, *Phys. Lett. B* **497** (2001) 281 [arXiv:hep-ph/0008205].
- [17] M. Malquarti, E. J. Copeland, A. R. Liddle and M. Trodden, *A new view of k-essence*, *Phys. Rev. D* **67** (2003) 123503 [arXiv:astro-ph/0302279].
- [18] S. Hannestad and E. Mörtsell, *Cosmological constraints on the dark energy equation of state and its evolution*, *JCAP* **0409**, 001 (2004) [arXiv:astro-ph/0407259].
- [19] M. Joyce, *On the expansion rate of the universe at the electroweak scale*, *Phys. Rev. D* **55**, 1875 (1997) [arXiv:hep-ph/9606223].
- [20] N. Arkani-Hamed, S. Dimopoulos and G. R. Dvali, *The hierarchy problem and new dimensions at a millimeter*, *Phys. Lett. B* **429**, 263 (1998) [arXiv:hep-ph/9803315],  
*Phenomenology, astrophysics and cosmology of theories with sub-millimeter dimensions and TeV scale quantum gravity*, *Phys. Rev. D* **59**, 086004 (1999) [arXiv:hep-ph/9807344].
- [21] L. J. Hall and D. R. Smith, *Cosmological constraints on theories with large extra dimensions*, *Phys. Rev. D* **60** (1999) 085008 [arXiv:hep-ph/9904267].
- [22] S. Hannestad, *Strong constraint on large extra dimensions from cosmology*, *Phys. Rev. D* **64** (2001) 023515 [arXiv:hep-ph/0102290].
- [23] P. Brax, C. van de Bruck, A. C. Davis, J. Khoury and A. Weltman, *Detecting dark energy in orbit: The cosmological chameleon*, [arXiv:astro-ph/0408415] and *Chameleon dark energy*, [arXiv:astro-ph/0410103].  
P. Brax, C. van de Bruck and A. C. Davis, *Is the radion a chameleon?*, *JCAP* **0411**, 004 (2004) [arXiv:astro-ph/0408464].
- [24] D. A. Dicus and W. W. Repko, *Constraints on the dark energy equation of state from recent supernova data*, *Phys. Rev. D* **70**, 083527 (2004) [arXiv:astro-ph/0407094].
- [25] I. Antoniadis, N. Arkani-Hamed, S. Dimopoulos and G. R. Dvali, *New dimensions at a millimeter to a Fermi and superstrings at a TeV*, *Phys. Lett. B* **436**, 257 (1998) [arXiv:hep-ph/9804398].

## Appendix A: Explicit Relation Between $\chi$ and $M_b r$

The defining relation for the  $\chi$ -field is:

$$(\partial\chi)^2 \equiv M_b^2 \left[ \frac{3}{2} \left( 2 + \frac{a}{A} \right)^2 - \frac{2B}{A} \right] (\partial \log M_b r)^2 \quad (7.1)$$

where the functions  $A$ ,  $B$  and  $C$  are given by (2.7-2.9). The function appearing in the square brackets can be written as a polynomial in  $\tilde{A} = A/a$ :

$$\begin{aligned} \mathbb{R} &= \frac{3}{2}(2A + a)^2 - 2AB \\ &= \alpha + \beta\tilde{A} + \gamma\tilde{A}^2, \end{aligned} \quad (7.2)$$

where

$$\alpha = \frac{3a^2}{2}, \quad \beta = 2(3a^2 - a + b), \quad \gamma = 2a(3a - b), \quad (7.3)$$

and

$$\Delta = 4\alpha\gamma - \beta^2. \quad (7.4)$$

We can now write (7.1) solely in terms of  $\tilde{A}$ :

$$(\partial\chi)^2 \equiv M_b^2 \frac{\mathbb{R}}{a^2 \tilde{A}^2} (\partial \tilde{A})^2. \quad (7.5)$$

The solution for this equation can be found by direct integration. For  $\beta$ ,  $\gamma$ ,  $\Delta \neq 0$  one finds

$$\frac{\chi}{M_b} = \frac{1}{|a|} \left( \sqrt{\mathbb{R}} - \sqrt{\alpha} \log \left| \frac{2\sqrt{\alpha\mathbb{R}} + \beta\tilde{A} + 2\alpha}{\tilde{A}} \right| + \frac{\beta}{2} \mathbb{X} \right) \times \operatorname{sgn} \tilde{A}, \quad (7.6)$$

where

$$\mathbb{X} = \begin{cases} \frac{1}{\sqrt{\gamma}} \log \left| 2\sqrt{\gamma\mathbb{R}} + 2\gamma\tilde{A} + \beta \right| & \text{for } \gamma > 0 \\ \frac{-1}{\sqrt{-\gamma}} \arcsin \frac{2\gamma\tilde{A} + \beta}{\sqrt{-\Delta}} & \text{for } \gamma < 0. \end{cases} \quad (7.7)$$

If  $\beta = 0$  the solution is instead

$$\frac{\chi}{M_b} = \frac{1}{|a|} \left( \sqrt{\mathbb{R}} - \sqrt{\alpha} \log \left| \frac{\sqrt{\mathbb{R}} + \sqrt{\alpha}}{\tilde{A}} \right| \right) \times \operatorname{sgn} \tilde{A}, \quad (7.8)$$

for  $\gamma = 0$  one finds

$$\frac{\chi}{M_b} = \frac{1}{|a|} \left( 2\sqrt{\mathbb{R}} + \sqrt{\alpha} \log \left| \frac{\sqrt{\mathbb{R}} - \sqrt{\alpha}}{\sqrt{\mathbb{R}} + \sqrt{\alpha}} \right| \right) \times \operatorname{sgn} \tilde{A}, \quad (7.9)$$

and finally for  $\Delta = 0$  the solution is

$$\frac{\chi}{M_b} = \frac{1}{|a|} \left( \sqrt{\gamma}\tilde{A} + \sqrt{\alpha} \log |\tilde{A}| \right) \times \operatorname{sgn} \left( \sqrt{\gamma} + \sqrt{\alpha}/\tilde{A} \right). \quad (7.10)$$

All of the above solutions are valid at least in the range  $-0.1 < a < 0.1$  and  $-0.1 < b < 0.1$ .